TOOLS TO IMPROVE DETECTION OF STRUCTURAL CHANGES FROM IN-FLIGHT FLUTTER DATA.

Marco Scionti*, Jeroen Lanslots[‡], Ivan Goethals[†], Antonio Vecchio[‡], Herman Van der Auweraer[‡], Bart Peeters[‡], Bart De Moor[†]

[‡] LMS International, TST Research & Technology Development, Researchpark Z1, Interleuvenlaan 68, B-3001, Leuven, Belgium
[†] ESAT-SCD KU Leuven, Department of Electronics, Kasteelpark Arenberg 10, B-3001 Leuven (Heverlee), Belgium
* Catania University, Department of Industrial and Mechanical Engineering, Viale A. Doria 6, 95125, Catania, Italy

Abstract. Airworthiness authorities require specific in-flight flutter testing be performed before flight certificates are granted to new aircraft. Flutter tests consist of flying the aircraft at different airspeeds to provide evidence that no unsafe aeroelastic phenomena show-up in the flight domain. Data collected through in-flight tests are then processed to extract eigenfrequencies and damping ratios in varying flight conditions to track the dynamical characteristics for different airspeed values. However, extracting modal parameters from in-flight tests generates a variety of inherent problems. This encompasses measurement noise, missing or noised excitation signals, and low number of sensors generating spatial aliasing.
Noisy data generate more spurious poles in stabilization diagrams; this in turn increases the difficulty to select stable poles (*pole-picking*) and to correctly identify mode shapes.
A new technique is presented based on energy considerations and a ruled-based pole-picking tool is introduced to improve the pole selection process. They allow detecting and removing mathematical poles from the stabilization diagram and speeding up the pole selection process. Furthermore, the first technique, when coupled with other techniques such as cluster analysis or fuzzy logic, provides a ranking for the pole selection, paving the way to the implementation of a tool to automatically select only physically meaningful poles.

1. INTRODUCTION

System identification is a standard tool for the analysis of forcefully or ambient excited vibrating structures [14]. A linear model for such a structure is built from available observations, based on which modal parameters as resonance frequencies, damping ratio and modal shapes can be estimated. To reduce the bias on the estimates and allow the model to capture all relevant characteristics of the structure, the identification order is usually chosen quite high. However, the higher the model order is chosen, the higher number of estimated poles will be calculated. This results in the occurrence of so-called spurious poles.

In this paper we will describe several mathematical methods that use a full state-space model that detect less relevant modes and remove them from the model, without reverting to a stabilization diagram (section 4).
On the other hand, there is an intelligent rule-based technique that does analyse the stabilization diagram selecting only the physical poles (section 5). This technique is based on a knowledge acquisition process that is observing skilled engineers, and has the advantage that less experienced people have access to knowledge from expert engineers. Furthermore, the method does not depend on the parameter estimation method used to obtain the stabilization diagram.
Although the techniques that are presented are generally heuristic by nature, we show by means of an example from the aerospace industry that in a practical case, a quick automated discrimination between spurious and physical modes can effectively be made.
In section 2 we show the basic concepts of state space models and the theory of balanced model reduction from a practical point of view. Section 3 describes the stochastic subspace Balanced Realisation method. In section 6 we compare the different mode selection techniques by means of data obtained from an in-flight flutter test of an airplane. We show that the presented methods can effectively be applied to detect and remove spurious modes from a linear model, even in the presence of large amounts of measurement noise. Finally, in section 7, some conclusions are drawn.

2. THE STATE SPACE FORMULATION AND BALANCING

We will consider state space models of the form:

$$\begin{aligned} x_{k+1} &= Ax_k + Bu_k + w_k, \\ y_k &= Cx_k + Du_k + v_k, \end{aligned} \tag{1}$$

with

$$E\left\{\begin{bmatrix} w_p \\ v_p \end{bmatrix}\begin{bmatrix} w_q^T & v_q^T \end{bmatrix}\right\} = \begin{bmatrix} Q & S \\ S^T & R \end{bmatrix}\delta_{pq} \geq 0, \tag{2}$$

where $E\{\cdot\}$ denotes the expected value operator and δ_{pq} the Kronecker delta. It is assumed that:

$$E\left\{\begin{bmatrix} w_p \\ v_p \end{bmatrix} x_k^T\right\} = 0, \forall p \geq k\,. \tag{3}$$

The elements of the vectors $y_k \in \mathbf{R}^l$ and $u_k \in \mathbf{R}^m$ are given observations of the outputs and inputs of the system at the discrete time index k. The vector $x_k \in \mathbf{R}^n$ is the unknown state vector at time k. The unobserved process and measurement noise $w_k \in \mathbf{R}^n$ and $v_k \in \mathbf{R}^l$ are assumed to be white, zero mean, gaussian with covariance matrices as given in (2). The system matrices A,B,C,D and the covariance matrices Q, S, and R have appropriate dimensions.
The state-space representation (1) is not unique. Applying a basis transformation $x \to Tx$ and a corresponding transformation of the state space matrices, $(A, B, C, D) = (TAT^{-1}, TB, CT^{-1}, D)$, the model (1) can be written in a multitude of forms, which all describe the same *input/output* behaviour. A common representation in modal analysis is the so-called modal representation,

$$\begin{aligned} x_{k+1}^m &= \Lambda x_k^m + B^m u_k + w_k, \\ y_k &= C^m x_k^m + D u_k + v_k, \end{aligned} \tag{4}$$

where the system matrix Λ is diagonal and mainly consists of pairs of complex conjugated eigenvalues $\lambda, \bar{\lambda}$ being the poles of the system. For this to be possible the original system matrix A needs to be diagonalizable which is in practical applications usually the case. The modal characteristics of the structure under study can then easily be obtained from (4) as follows:

$$\begin{aligned} f_i &= \arg\left(\lambda_i \tfrac{T_s}{2\pi}\right), \\ d_i &= \frac{\ln\left(|\lambda_i|\right)}{\sqrt{\ln\left(|\lambda_i|\right)^2 + \arg\left(\lambda_i\right)^2}}, \\ v_i &= C^m(:, i), \end{aligned} \tag{5}$$

with f_i, d_i and v_i the resonance frequency, damping and mode shapes corresponding to the i^{th} pole $\Lambda(i, i) = \lambda_i$. T_s is the sampling rate.

Another commonly used representation is the so-called Balanced Representation [11]. The idea of the Balanced Representation is to decompose the controllability and observability grammians of the model into principal components in order to evaluate the contributions of each mode to the overall *input/output* behaviour of the model. The controllability grammian P and observability grammian Q can easily be obtained as solutions to the following Lyapunov equations:

$$\begin{aligned} APA^T + P - BB^T &= 0, \\ A^T QA + Q - C^T C &= 0. \end{aligned} \tag{6}$$

The key property of a balanced realization is that a state transformation $x^b = Tx$ and a corresponding similarity transformation $(A^b, B^b, C^b, D) = (TAT^{-1}, TB, CT^{-1}, D)$ is selected such that the both grammians are equal to a diagonal matrix Σ.

$$\begin{aligned} A^b \Sigma A^{bT} + \Sigma - B^b B^{bT} &= 0, \\ A^{bT} \Sigma A^b + \Sigma - C^{bT} C^b &= 0. \end{aligned} \tag{7}$$

The larger a diagonal entry of the grammians, the bigger the contribution of the corresponding entry of the state vector to the overall *input/output* behaviour of the model. The diagonal entries are therefore usually sorted on the diagonal in descending order. The so-called concept of Balanced model reduction is then nothing else than the removal of the last entries of the state. More concretely, if the balanced system matrices are partitioned as follows:

$$A^b = \begin{bmatrix} A_{11}^b & A_{12}^b \\ A_{21}^b & A_{22}^b \end{bmatrix}; \; B^b = \begin{bmatrix} B_1^b \\ B_2^b \end{bmatrix}; \; C^b = \begin{bmatrix} C_1^b & C_2^b \end{bmatrix}. \tag{8}$$

The reduced model would be $(A_{11}^b, B_1^b, C_1^b, D)$.

3. BALANCED REALISATION OUTPUT/ONLY DATA METHOD

The *output/only* time domain stochastic subspace Balanced Realisation (BR) is based on the following stochastic model derived from model (1) where the input signals were removed:

$$\begin{aligned}\{x_{k+1}\} &= [A]\{x_k\} + \{w_k\},\\ \{y_k\} &= [C]\{x_k\} + \{v_k\}.\end{aligned} \tag{9}$$

As measurement data, the response signals from a set of transducers are first processed into cross-correlations with respect to a pre-selected set of responses signals chosen as references. The key element of the method is the establishment and decomposition of the block Hankel matrix of these measured correlation functions. Let us define the empirical unbiased correlation matrix of the measured discrete output vector as:

$$[R_m] = \frac{1}{N-|m|}\sum_{t=0}^{N-|m|-1}\{y_{k+m}\}\{y_k\}^T, \tag{10}$$

where $\{y_k\}$ is the discrete output vector at time instant $k = 0...N-1$ and m is the time lag in terms of number of samples. Then the following block Hankel matrix can be defined and decomposed into its singular values:

$$[H_{p,p}] = \begin{bmatrix} [R_1] & [R_2] & \cdots & [R_p] \\ [R_2] & [R_3] & \cdots & [R_{p+1}] \\ \vdots & \vdots & \ddots & \vdots \\ [R_p] & [R_{p+1}] & \cdots & [R_{2p-1}] \end{bmatrix} = \begin{bmatrix}[U_1] & [U_2]\end{bmatrix}\cdot\begin{bmatrix}[S_1] & 0 \\ [0] & [S_2]\end{bmatrix}\cdot\begin{bmatrix}[V_1^T] \\ [V_2^T]\end{bmatrix}, \tag{11}$$

where

$$S_1 = diag(\sigma_1 \cdots \sigma_n), \sigma_1 \geq \sigma_2 \cdots \sigma_n \geq 0 \quad S_2 = diag(\sigma_{n+1} \cdots \sigma_{pN_{resp}})_n \text{ with } \sigma_{n+1} \rangle\rangle \sigma_n, \tag{12}$$

p is the so-called model order and it is a user defined parameter chosen so that $p>2N_m$, where N_m represents the number of physical modes; $[S_1]$ and $[U_1]$ contain respectively the n first singular values and the corresponding left singular vectors. From the stochastic realization theory, $[H_{p,p}]$ can be factored out as $[H_{p,p}] = [O_p]\,[C_p]$, and hence an estimate of the observability matrix is given by $[O_p] = [U_1][S_1]^{1/2}$. Therefore, considering that along with the modal model (9), the observability matrix $[O_p]$ and the controllability matrix $[C_p]$ of order p are defined:

$$[O_p] = \begin{bmatrix}[C] \\ [C][A] \\ \vdots \\ [C][A]^{p-1}\end{bmatrix}; [C_p] = \begin{bmatrix}[G] & [A][G] & \cdots & [A]^{p-1}[G]\end{bmatrix} \tag{13}$$

where $[G] = E[\{x_{k+1}\}\{y_k\}^T]$, the system matrices $[A]$ and $[C]$ are estimated up to similarity transformation, using the shift structure of $[O_p]$ [2] and using only the output measurements $\{y_k\}$. This identification problem is also known as the stochastic realization problem [2], [5]. Once the matrices $[A]$ and $[C]$ are estimated, the modal parameters could be easily determined by means of an eigenvalue decomposition $[A] = [\Phi][\Lambda][\Phi]^{-1}$. Complex eigenvectors and eigenvalues in the previous equation always appear in complex conjugate pairs. The discrete eigenvalues λ_r on the diagonal of $[\Lambda]$ can be transformed into continuous eigenvalues or system poles μ_r by using the following equation:

$$\lambda_r = e^{\mu_r \cdot \Delta t} \Rightarrow \mu_r = \sigma_r + j\varpi_r = \frac{1}{\Delta t}\ln(\lambda_r), \tag{14}$$

The mode shape $[\Psi]_r$ of the r-th mode at the sensor locations are the observed parts of the system eigenvectors $\{\Phi\}_r$ of the $[\Phi]$, given by the expression $\{\Psi\}_r = [C]\,\{\Phi\}_r$. Note that the extracted mode shapes cannot be mass-normalized, as this requires the measurement of the

input force. A full review of stochastic system identification methods for experimental modal analysis is presented in [12] and [13].

4. STATE SPACE BASED MATHEMATICAL POLE SELECTION METHODS

Introduction. In this section we will describe some mode selection techniques to remove spurious modes from a model of the form (1). We will thereby make extensive use of the modal and balanced representations of a system, introduced in section 2.

H_2 and H_∞ modal truncation. A first naïve approach would be to write the model in its modal form, as given in (4), remove a certain mode, and assess the "damage" done to the model in H_2 and H_∞ norm. Hence, if the full order model is called H_{full}, and H_{reduced} is the lower order model formed by removing the complex conjugated poles λ_i and $\overline{\lambda}_i$ from (4), the following expressions are evaluated:

$$\left\| H_{\text{full}} - H_{\text{reduced}} \right\|_2, \quad \left\| H_{\text{full}} - H_{\text{reduced}} \right\|_\infty, \tag{15}$$

where

$$H_{\text{full}}(z) - H_{\text{reduced}}(z) = \left[C^m(:,i) \quad \overline{C^m(:,i)} \right] \cdot \left(zI_2 - \begin{bmatrix} \lambda_i & 0 \\ 0 & \overline{\lambda}_i \end{bmatrix} \right)^{-1} \begin{bmatrix} B^m(i,:) \\ \overline{B^m(i,:)} \end{bmatrix}. \tag{16}$$

The expressions in (15) can be calculated as:

$$\begin{aligned} \left\| H_{\text{full}} - H_{\text{reduced}} \right\|_2 &= Tr\left(C(:,i) P_i C(:,i)^T \right), \\ \left\| H_{\text{full}} - H_{\text{reduced}} \right\|_\infty &= \max_\omega \overline{\sigma}\left(H_i(e^{j\omega}) \right), \end{aligned} \tag{17}$$

where P_i is the controllability matrix of the second order model (16), and can be obtained by solving Lyapunov equations as in (6). Numerical procedures are widely available for the calculation of the infinity norm [3]. After repeatedly calculating (17), once for each mode, the distance measures obtained are divided by their maximum value, this is, the maximum distance that can be obtained by removing 1 mode. The result is a number between 0 and 1 for each mode and each criterion (H_2 and H_∞) that was used as a significance parameter describing the importance of the mode.

In general it seems reasonable to assume that the more important a mode is, the bigger will be the influence of its removal from the model, and hence its significance parameter. Furthermore it is shown in [8] that for nearly undamped structures, the grammians of the modal form are almost diagonal, meaning that the modal and the balanced form are 'close' to each other in some sense. Hence, for such structures, modal truncation makes perfect sense since it leads to similar results as balanced model reduction. In many practical cases, however, the structure under study is not nearly undamped, and modal truncation may lead to an inadequate rejection of spurious mode due to phenomena as mode coupling, which make it very hard to assess the importance of a mode by examining a single second order subsystem. This will also be shown in the examples in section 4. In order to draw better conclusions for complicated structures, we will have a look into the connection between the balanced and the modal representation of the identified model.

Connection between the balanced and the modal form. Since the balanced and the modal form are both representations of the same model, there is always a similarity transformation T linking one form to the other:

$$\Lambda = TA^bT^{-1}\ B^m = TB^b \quad C^m = C^bT^{-1} \quad D^m = D^b\ . \tag{18}$$

From $\Lambda=TA^bT^{-1}$ it follows that the diagonal elements of Λ can be written as a linear combination of the entries of A^b, where we know that the entries of A^b that are most relevant for the *input/output* behaviour of the model are situated in its upper left part. A formal way to exploit this fact in a mode selection context is to replace A^b with a significance matrix S of the same dimensions, where the elements of S give a measure of the importance of the corresponding entries in A^b, e.g.

$$S = \begin{bmatrix} n & n-1 & n-2 & \cdots \\ n-1 & n-1 & n-2 & \cdots \\ n-2 & n-2 & n-2 & \cdots \\ \vdots & \vdots & \vdots & \ddots \end{bmatrix}, \tag{19}$$

and inspect the diagonal elements of $|T|\cdot S\cdot|T^{-1}|$, with $|T|$ the element wise absolute value of T, to obtain a measure for the significance of the corresponding pole in Λ. Again, the significance parameters are rescaled so as to lie between 0 and 1.

Continuous extension to balanced truncation. Closely related to the former technique is the concept of a continuous extension to balanced truncation. Instead of truncating the model and completely removing the last entries of the state, one might opt to change the balanced system matrix,

$$A^b = \begin{bmatrix} a^b_{11} & a^b_{12} & \cdots & a^b_{1n} \\ a^b_{21} & a^b_{22} & \cdots & a^b_{2n} \\ \vdots & \vdots & & \vdots \\ a^b_{n1} & a^b_{n2} & \cdots & a^b_{nn} \end{bmatrix}, \tag{20}$$

and introduce a small parameter ε to continuously remove the last entries of the state, e.g. as follows:

$$\widetilde{A}^b(\varepsilon) = \begin{bmatrix} a^b_{11} & \varepsilon a^b_{12} & \cdots & \varepsilon^{n-1}a^b_{1n} \\ \varepsilon a^b_{21} & \varepsilon a^b_{22} & \cdots & \varepsilon^{n-1}a^b_{2n} \\ \vdots & \vdots & & \vdots \\ \varepsilon^{n-1}a^b_{n1} & \varepsilon^{n-1}a^b_{n2} & \cdots & \varepsilon^{n-1}a^b_{nn} \end{bmatrix}. \tag{21}$$

While ε is continuously decreased, starting from one, the influence on the system poles can be assessed, e.g. by using the Euclidean distance measure in the complex plane. Again it is assumed that modes that are mainly related to the least important elements of A^b will be influenced more and can hence be classified as spurious.

Pole/zero cancellations. Pole/zero cancellations means that a zero of a rational entry in the transfer function matrix is almost or completely equal to a system pole. This renders a mode nearly uncontrollable or unobservable with respect to some or all of the inputs and outputs. Pole/zero cancellations are not uncommon in models identified from vibrating structures, especially when a high model order is used. Next to this, they are often an indication that the

cancelled pole is spurious. It is however seldom a good idea to take the distance between a pole and some nearby transfer function zeros as the basis of mode selection techniques. Lowly damped, weakly excited modes may well be accompanied by a nearby zero, even if the mode is quite important for the physical characteristics of the structure as a whole.
In [16], it was therefore proposed to take into account extra statistical information, such as the variance of a pole, when examining pole/zero cancellations. One of the techniques described in this work is to construct a confidence region around every pole and count the number of transfer function zeros within this region. Such confidence regions are not available if the model is obtained using subspace identification. It is however reasonably acceptable that if we started moving a pole in our model, the influence on the model as a whole would be inversely proportional to the variance on the pole position.
As a mode selection rule, similar to the one presented in [16] we therefore propose to move each pole to its $m \times l$ closest transfer function zeros and assess the influence on the model as a whole in each of the $m \times l$ cases, e.g. by calculating the sum of the 2- or infinity-norms of the differences between the adjusted and the original models. As usual, a significance parameter is obtained by dividing the determined distances by their maximum, resulting in a value between 0 and 1.

Cross correlations with SISO models. An obvious criterion, proposed in [16], is to check to what extent poles of the full MIMO model (1) can be retrieved from smaller models obtained from individual or groups of input and output sequences. For our example in section 4, we constructed l MISO models from the available observations, one for each output, and compared the obtained poles with the ones from the full MIMO model using the standard Euclidean distance measure in the complex plain. To speed up the procedure, the individual models can for instance be obtained using a fast ARX modelling procedure.

5. RULE-BASED TECHNIQUE FOR AUTOMATIC POLE SELECTION

Introduction. This section describes a rule-based intelligence approach to separate the spurious modes from the physical ones in stabilization diagrams [10] according to [9]. This has lead to the development of a tool (AASD), which will be used in the evaluation, section 6.

Rule-based intelligence. The automatic assessment of stabilization diagrams is modelled on the knowledge of a human engineer. Engineers normally assess stabilization diagrams, obtained by applying BR, LSCE [4], or other parameter estimation methods [6], [7], by visually inspecting them on screen, hereby using knowledge and experience. The visual information that is present to the engineer consists of the symbols in the stabilization diagrams, which are based on similarity in frequency, damping ratio and/or mode vectors between poles belonging to subsequent model orders [10]. Based on these sources of information, the engineer selects a number of poles by hand. In a later step, this handpick could be checked with validation tools such as the Modal Assurance Criterion (MAC) [1].
Knowledge acquisition was done by observing engineers performing this task. The next step was transforming these observations into a deterministic set of rules to ensure that the same stabilization diagram is always assessed in exactly the same way. In general, the observations lead to the conclusion that an engineer first selects a vertical column of poles. Then, the subsequent poles in that column are assessed based on the variance in frequency and damping ratio. Based on that, a certain pole will be selected, or the column will be disregarded.

Column selection. To select a vertical column, we used a double set of histograms, one shifted by half a bin-width. The width of the histograms bins was left as a parameter to be set, as this can change according to the density of the stabilization diagram under assessment. In practise though, a bin-width between 0.5% and 1.0% of the maximum frequency is sufficient.
On each of these bins a number of rules will be applied, called *Euclidian distance*, S*table poles*, and *Neighbouring bins,* resulting in a score for each bin.

Euclidian distance. This procedure calculates a weight for every bin. It first calculates the Euclidian distance E_d of the frequencies of every pole in that bin with respect to the centre frequency of that bin. Then a comparison is made with the Euclidian distances of all the other bins. Based on this comparison, a weight is calculated for each bin, which stands for how well that column of poles is aligned. Thus, this step tries to mimic what the human engineer is doing visually by looking at a monitor. Furthermore, it not only accepts or rejects a bin as the engineer would do, but also gives a score as to how well aligned that bin actually is.

Stable poles. When engineers assess stabilization diagrams, they are especially looking for *s*-type poles. In LMS software such as *Cada-X* and its successor *Test.Lab*, an *s*-type pole denotes a pole that is stable in frequency (default 1%), damping ratio (default 5%) and mode vector (default 2%) with respect to a pole at the previous model order [10].
The *Stable poles* step gives a weight to a bin based on the occurrence of these *s*-type poles, based on a logarithmic function of the number of stable poles in a bin. Although also left to be set as a parameter a default value of 3 stable poles is used, meaning that the appearance of more poles is not greatly rewarded, but that the absence of poles is punished.

Neighbouring bins. The weights resulting from the *Euclidian distance* and *Stable poles* procedures are multiplied by the histogram values of the bins. But, because every pole exists in two bins – the normal one and the shifted one – a choice still has to be made. For that, a procedure called *Neighbouring bins* was introduced, which decides locally for every normal bin whether it will choose that one, or its shifted left or right neighbour. Bins that have a score below $^1/_3$ of the model order (this threshold is a user-defined parameter) are disregarded altogether. This enables for all bins a local decision as to how good they are.

Pole-picking. Now, a number of bins have been selected. Each of these bins is considered centred around the frequency of a physical pole. Thus, from each bin, the best pole has to be picked. First of all, it was decided that such a pole should always be an *s*-type pole. Bins without *s*-type poles are therefore discarded. When observing an engineer doing this pole-picking by hand, he will look for a sequence of *s*-type poles and choose one of them if their damping ratios are sufficiently constant. The *pole-picking* procedure was introduced here to capture this human skill. It consists of a clustering part that clusters the poles in each bin according to their damping ratios. Then the best cluster is picked, and from that cluster, the best pole is determined. This pole is considered as the pole that the human expert engineer would pick by hand, comparing damping ratios, and using expert knowledge.

Double Poles. Based on the procedure described so far, it would not be possible to detect double poles. By a double pole is meant the existence of two poles at almost exactly the same frequency, at the same model order, with sometimes the same damping ratio, but in any case with a different mode vector.
For the detection of double poles it was therefore decided to introduce mode vector information just after the creation of the histograms. This approach turns the two-dimensional problem (frequency, damping) into a three-dimensional one (frequency, damping, mode

vector) by means of which new features of the data might be detected. For that, all the *s*-type poles in one bin are clustered according to their MAC-value. If multiple clusters occur within one bin, it is considered to contain a double pole and is further assessed in a way similar to the *pole-picking* procedure, hereby using damping ratio and a score for the number of *s*-type poles in each cluster. If this is above a threshold of $^1/_3$ of the model order, it is considered a double pole. The rest is discarded as being non-physical phenomena.

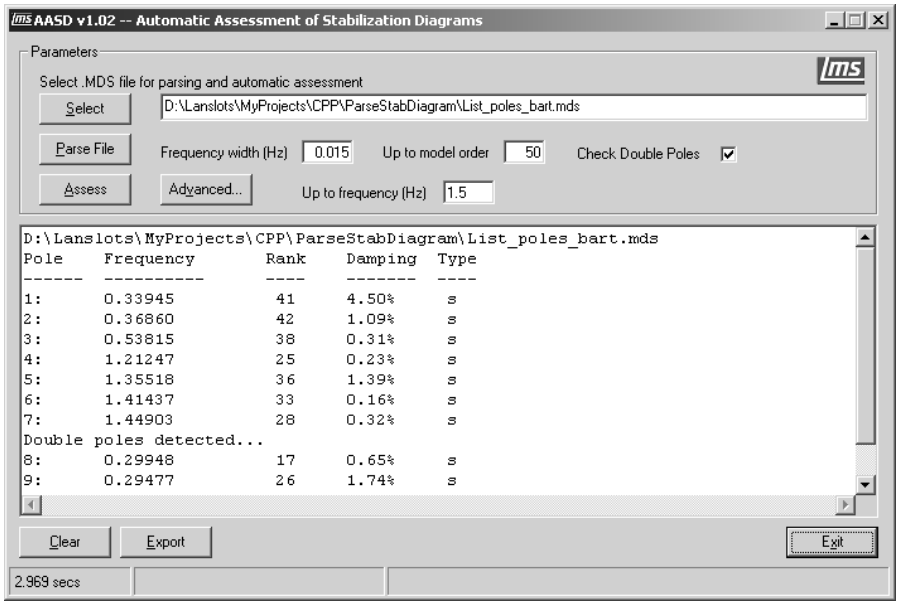

Figure 1: AASD tool screenshot

AASD Tool. The above procedure was processed into a software tool called AASD (Automatic Assessment of Stabilization Diagrams), of which a screenshot can be viewed in figure 1. As already noted, a number of parameters were introduced with default values. All of these default values can be changed according to need.

6. EVALUATION

Introduction. In order to evaluate the techniques outlined in sections 5 and 6, we will apply them to a dataset, consisting of observation data acquired from an in-flight flutter test of an aircraft. It can be analysed as *input/output* data when considering the input as being white noise introduced in the flight control system, in the 0–60 Hz frequency range. On the other hand, it can also be analysed as *output/only* data disregarding the input, since, in many cases, it is not available in an in-flight dataset due to measurement difficulties. In the latter case the rule-based technique will be applied on the BR stabilization diagram so as to assess its performances when compared with the state space method, applied here on *input/output* data, coupled with the same rule-based pole-picking technique.

In-Flight flutter testing of an aircraft. The dataset consists of 67 seconds of measurement data, sampled at 256 Hz, obtained during in-flight flutter tests of a fly-by-wire airplane equipped with 13 sensors, one of which is the input, injected as white noise in the electronics of the plane. This dataset was analysed with two different parameter estimation methods. First considering the input signal, the data were analysed using a robust N4SID subspace algorithm, described in [15]. Then, assuming an *output/only* dataset, the *Cada-X* BR

operational algorithm was used. Figure 2 and 3 show the stabilization diagrams obtained with the N4SID and BR parameter estimation method.

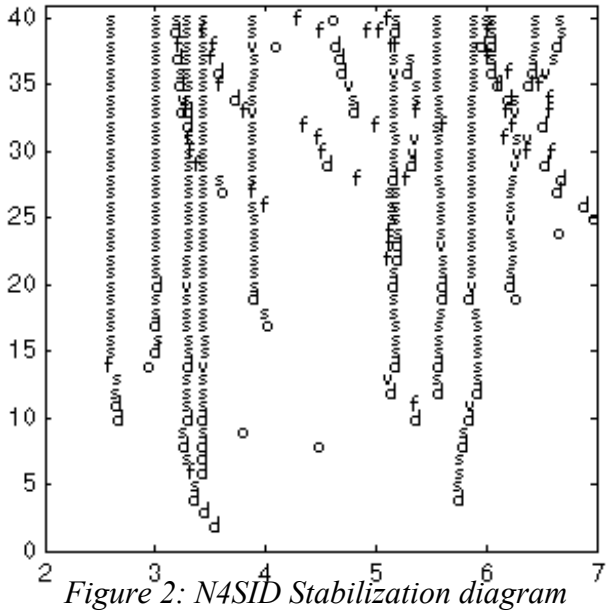

Figure 2: N4SID Stabilization diagram

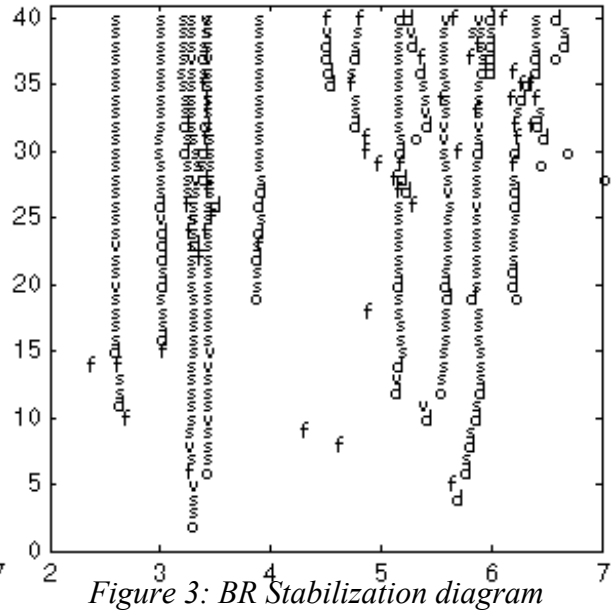

Figure 3: BR Stabilization diagram

Table 1 shows the results calculated by using the two different estimation methods and pole-picking techniques. The first column presents the results obtained by the *input/output* state space based pole-picking methods (sections 2 and 4). Seven modes were found to be significantly more relevant in a sorted list of poles. In practice, determining this number of relevant modes often requires some human judgement as it is not always clear where the relevance threshold should be set. The empty row in column 1 does not mean that no mode has been found at that frequency, but only that the relevance score indicated that the mode is relatively less important, and thus marked as spurious (score 0.421 at 3.9 Hz).

N4SID/State space		***N4SID/Rule-based***		***BR/Rule-based***	
Freq	***Damp***	***Freq***	***Damp***	***Freq***	***Damp***
2.609 Hz	**2.53%**	**2.609 Hz**	**2.52%**	**2.602 Hz**	**3.04%**
3.006 Hz	**3.05%**	**3.004 Hz**	**3.17%**	**2.981 Hz**	**2.68%**
3.296 Hz	**4.92%**	**3.296 Hz**	**4.83%**	**3.275 Hz**	**5.67%**
3.439 Hz	**2.75%**	**3.440 Hz**	**2.65%**	**3.444 Hz**	**2.30%**
x	**x**	**3.903 Hz**	**4.22%**	**3.924 Hz**	**1.17%**
5.179 Hz	**2.73%**	**5.173 Hz**	**2.89%**	**5.173 Hz**	**3.14%**
5.590 Hz	**2.77%**	**5.578 Hz**	**3.06%**	**5.569 Hz**	**1.15%**
5.901 Hz	**4.09%**	**5.881 Hz**	**3.56%**	**5.944 Hz**	**2.63%**

Table 1: Selected modes

The second column gives the selected modes based on the rule-based pole-picking method applied on the stabilization diagram of the N4SID method (sections 2 and 5). The third column gives the selected modes as they were detected using the stochastic subspace based BR method for *output/only* data, coupled with the rule-based tool (sections 4 and 5).
Note that the mode at 3.9 Hz is stabilized in figure 2, but was not accepted as such by our *input/output* state space pole-picking methods (sections 2 and 4). However, since it is clearly visible in the diagram (figure 2), it was detected by the AASD tool. Also note that some of the damping ratios in the third column differ from those in the first and second column; in

general, the missing input information turns into a more difficult parameter estimation process as is clearly recognizable by comparing the stabilization diagrams of figures 2 and 3.
Finally, the dataset was also analysed by experts of the aircraft's manufacturer. They confirmed the results presented in table 1.

7. CONCLUSIONS

When analysing the results obtained by the state space approach, it was observed that the H_2 and H_∞ criterion of section 4 for the modes at 2.6 and 3 Hz indicated weak excitation. This also shows that simple modal truncation is not suited for the analysis of complicated structures. On the other hand, the algorithm based on the connection between the modal form and the balanced form performed quite well and is, together with the cross correlation, probably the best method to use for mode selection by the state space approach; this despite the fact that not all physical modes were detected.
The rule-based technique (section 5) proved very useful for stabilization diagrams obtained by the N4SID method. It found proof for the selection of one more mode (at 3.9 Hz), which was already pointed out as a tricky one by the airplane manufacturer's experts. It is also clearly visible in the stabilization diagram of figures 2 and 3.
From this it can be stated that the combination of N4SID and the rule-based intelligence is very promising. Together they performed a modal analysis and succeeded with presenting a well-fit model from very noisy in-flight data of a complicated structure such as the aircraft under examination.

Next, the rule-based technique was applied on a lower quality stabilization diagram, obtained with *output/only* data. Despite the lack of input-information, we still succeeded in obtaining an acceptable set of modes. A good modal model can still be defined which is consistent with the results obtained with the *input/output* N4SID method.
It can thus be concluded that the rule-based technique is a flexible tool that performs quite well when applied to any parameter estimation method that results in a stabilization diagram.

8. ACKNOWLEDGEMENTS

This research was carried out in the context of the EUREKA project E!2419 "FLiTE". This work was also made possible under the European Commission research project IST Marie Curie Industry Host Fellowship 'DIMENSION' (Jeroen Lanslots). The EC, Catania University (DIIM) and the IWT are greatly acknowledged for their support.

KUL research is supported by grants from several funding agencies and sources: **Research Council KUL:** Concerted Research Action GOA-Mefisto 666, IDO, several PhD/postdoc & fellow grants; **Flemish Government:** Fund for Scientific Research Flanders (several PhD/postdoc grants, projects G.0256.97, G.0115.01, G.0240.99, G.0197.02, G.0407.02, research communities ICCoS, ANMMM), AWI, IWT (Soft4s, STWW-Genprom, GBOU-McKnow, Eureka-Impact, Eureka-FLiTE, several PhD grants); **Belgian Federal Government:** DWTC (IUAP IV-02 (1996-2001) and IUAP V-22 (2002-2006)), PODO-II (CP/40); **Direct contract research:** Verhaert, Electrabel, Elia, Data4s, IPCOS.

REFERENCES

1. Allemang, R.J., and Brown, D.L., A Correlation Coefficient for Modal Vector Analysis. In *Proceedings of International Modal Analysis Conference*, 110–116, 1982.
2. Basseville, M., Benveniste, A., Goursat, M., Hermans, L., Mevel, L., and Van Der Auweraer, H., *Output/only* Subspace-Based Structural Identification: From Theory to Industrial Testing Practice, In *ASME J. of Dyn. Systems, Meas. And Control*, 123(4), (in press), 2001.
3. Boyd, S., Balakrishnan, K., and Kabamba, P., A bisection method for computing the H_∞ norm of a transfer matrix and related problems. In *Mathematics of Control, Signals and Systems,* 2(3), 1989, 207–219.
4. Brown, D.L., Allemang, R.J., Zimmerman, R., and Mergeay, M., Parameter Estimation Techniques for Modal Analysis. *SAE-paper 790221*, 19, 1979.
5. Desai, U., Debajyoti, P., and Kirkpatrick, R., A realization approach to stochastic model reduction, In *Int. J. Control*, vol. 42, no. 4, 1985, 821–838.
6. Ewins, D.J., *Modal Testing. Theory, practise and appliction. Second Edition.* Research Studies Press Ltd., Baldock, Hertfordshire, England, 2000.
7. Heylen, W., Lammens, S., and Sas, P., *Modal Analysis Theory and Testing.* Katholieke Universiteit Leuven, Department of Mechanical Engineering, PMA, Leuven (Heverlee), Belgium, 1997.
8. Jonckheere, E.A., Principal Component Analysis of Flexible Systems – Open loop case. In *IEEE Trans. Automat. Contr.,* 1984, vol. AC-29, No 12, december, 382–38.
9. Lanslots, J.P., and Scionti, M., Automatic Assessment of Stabilization Diagrams. Technical Report, LMS International, TST Technology Deployment & Research, Leuven, Belgium, October 2002.
10. LMS International, *Cada-X* Manuals Rev 3.5.D – Modal Analysis. LMS International, Leuven, Belgium, 2002.
11. Obinata, G., and Anderson, B.D.O., *Model Reduction for Control System Design*. Springer-Verlag, London, 2001.
12. Peeters, B., *System Identification and Damage Detection in Civil Engineering,* PhD thesis, Department of Civil Engineering, K.U. Leuven, Belgium, [`http://www.bwk.kuleuven.ac.be/bwm`], December 2000.
13. Peeters, B., and De Roeck, G., Stochastic system identification for operational modal analysis: a review. In *ASME Journal of Dynamic Systems, Measurement, and Control*, 123(4), 2001, 659–667.
14. Van der Auweraer, H., Structural Dynamics Modeling using Modal Analysis: Applications, Trends and Challenges, in H. Van der Auweraer, editor, *Proceedings of the 2001 IEEE Instrumentation and Measurement Technology Conference*, Budapest, Hungary, 2001.
15. Van Overschee P., and De Moor, B., *Subspace Identification for Linear Systems: Theory – Implementation – Applications*. Kluwer Academic Publishers, Boston/ London/Dordrecht, 1996.
16. Verboven, P., Parloo, E., Guillaume, P., and Van Overmeire, M., Autonomous Structural Health monitoring. Part 1: Modal Parameter Estimation and Tracking. *Mechanical Systems and Signal Pocessing* (In Press), 2002.